European Journal of Radiology 120 (2019) 108609

Contents lists available at ScienceDirect

European Journal of Radiology

journal homepage: www.elsevier.com/locate/ejrad

Research article

Improving survival prediction of high-grade glioma via machine learning techniques based on MRI radiomic, genetic and clinical risk factors

Yan Tan[a,b,1], Wei Mu[a,1], Xiao-chun Wang[a,b], Guo-qiang Yang[a,b], Robert James Gillies[c,**], Hui Zhang[a,b,*]

[a] Department of Radiology, First Clinical Medical College, Shanxi Medical University, Taiyuan 030001, Shanxi Province, China
[b] College of Medical Imaging, Shanxi Medical University, Taiyuan 030001, Shanxi Province, China
[c] Departments of Cancer Physiology, H. Lee Moffitt Cancer Center and Research Institute, Tampa, Florida, USA

ARTICLE INFO

Keywords:
High grade glioma
Radiomics
Genetic risk factor
Clinical risk factor
Overall survival

ABSTRACT

Objectives: To develop a radiomic signature to predict overall survival (OS) for high-grade glioma (HGG), and construct a nomogram by combining selected radiomic, genetic and clinical risk factors to further improve the performance of the risk model.

Materials and Methods: 147 cases of HGG with MRI images, genetic data, clinical data were studied, wherein 112 patients were used as training cohort, and 35 patients were as independent test cohort. Radiomics features were extracted from tumor area and peritumoral edema area on CE-T1WI and T2FLAIR images. Association between radiomics signature, genetic, clinical risk factors and OS was explored by Kaplan-Meier survival analysis and log rank test. The multivariate Cox regression analysis was trained with radiomic features along with selected genetic and clinical risk factors, which was presented as a nomogram.

Results: The radiomic signature constructed by 11 radiomics features stratified patients into low- and high-risk groups, and the C-Index for OS prediction was 0.707 and 0.711 in training and test cohorts, respectively. The multivariable Cox regression analysis identified radiomics signature (hazard ratio (HR): 2.18, $P = 0.005$), IDH (HR: 0.490, $P = 0.007$) and age (HR: 1.039, $P = 0.005$) as independent risk factors. A nomogram combining these independent risk factors further improved the performance for OS estimation (C-index = 0.764 and 0.758 in training and test cohorts, respectively).

Conclusion: The radiomics signature is a new prognostic biomarker for HGG. A nomogram incorporating radiomics signature, IDH and age improved the performance of OS estimation, which might be a new complement to the treatment guidelines of glioma.

1. Introduction

High-grade gliomas (HGG) defined as a WHO Grade III-IV diffuse glioma are highly aggressive primary cerebral tumors with dismal prognoses [1]. Currently, standard comprehensive treatments including maximum surgical resection followed by adjuvant chemoradiotherapy are widely adopted for HGG [2,3]. The median overall survival (OS) for Grade III and IV glioma is 24 months and 14 months [1,4], respectively. However, in clinical practice, the OS of patients with HGG may differ significantly for each other though the patients have the same pathological grade and receive similar treatments [5–7]. The wide spectrum of OS existing in HGG underscores the imperative need for personalizing treatment options [8]. Stratification of clinical groups will directly impact image-guided diagnosis and subsequence treatment options for glioma. Therefore, identifying effective prognostic factors which stratified the clinical groups could help inform individualized management strategies and improve the prognosis of HGG.

Compared to qualitative analysis made by radiologists [9,10], radiomics based on machine learning method could provide more quantitative imaging biomarkers of prognostic assessment for glioma [11–14]. Furthermore, estimations based on multivariable model is considered more reliable for prognostic analyses [15]. Currently, many studies have identified other prognostic factors for gliomas, including clinical risk factors (age, gender, Karnofsky performance status, the

* Corresponding author at: Department of Radiology, First Clinical Medical College, Shanxi Medical University, Taiyuan 030001, Shanxi Province, China.
** Corresponding author at: Department of Cancer Physiology, H. Lee Moffitt Cancer Center and Research Institute, 12902 Magnolia Drive, Tampa, 33612 FL, USA.
E-mail addresses: Robert.Gillies@moffitt.org (R.J. Gillies), zhanghui_mr@163.com (H. Zhang).
[1] These two authors contributed equally to this work.

https://doi.org/10.1016/j.ejrad.2019.07.010
Received 26 April 2019; Accepted 8 July 2019

extent of resection) [1,16] and genetic risk factors [Oxygen 6-methylguanine-DNA methyltransferase gene promotor methylation (MGMTmet), isocitrate dehydrogenase mutation (IDH-M), and deletion of 1p/19q [1]] [17–20]. Using one risk factor alone to predicting prognosis is challenging due to the heterogeneity of gliomas. Using a multivariable model based on the comprehensive integration of radiomics signature, genetic and clinical risk factors to analysis the survival of HGG might be a more effective and reliable way.

Hence, the aim of the present study was to develop and externally validate a radiomic signature extracted from multiparametric and multiregional MRI images for predicting prognosis; and to develop a risk stratification model for HGG by construct a nomogram that combines radiomic signature, genetic and clinical risk factors.

2. Materials and methods

2.1. Patients

In this study, a total of 147 patients with pathologically confirmed HGG were included: 112 were selected from The Cancer Imaging Archive (TCIA) database and used as training cohort, and 35 were collected from *** hospital according to inclusion and exclusion criteria (Supplementary S1 and Supplementary Fig. 1) and used as an independent test cohort. As TCIA are publicly available database without patient identifiers, no institutional review board approval was required for the training cohort. For the independent test cohort, the institutional review board of *** university approved the study protocol. Given the retrospective study and anonymized patient data, informed consents were waived.

The information of IDH-M and MGMTmet in the training cohort was obtained from The Cancer Genome Archive (TCGA). In the test cohort, IDH-M was determined using Sanger sequencing, the MGMTmet was determined by pyrosequencing analysis, all the details of IDH-M and MGMTmet detection are shown in Supplementary S2.

Baseline clinical data including age, gender, histologic grade (Grade III and Grade IV), treatment and OS were obtained from the medical records. OS was calculated from the initial pathologic diagnosis date to death or censure point if still alive. The minimum follow-up period to ascertain the OS was 24 months after the initial pathologic diagnosis if patients were alive.

The flowchart of this study is shown in Fig. 1.

2.2. MRI data acquisition and process

MR images acquisition for the test cohort: preoperative MRI was performed with a 3.0-T scanner (GE Signa HDxt) using an 8-channel array coil. Radiomic features were extracted from both contrast-enhanced T1-weighted imaging (CE-T1WI) and T2 fluid-attenuated inversion recovery (T2FLAIR) images. The parameters were repetition time (TR) 195 ms and echo time (TE) 4.76 ms for gradient-echo (GRE) CE-T1WI; TR 8000 ms, TE 95 ms, and inversion time (TI) 2000 ms for T2FLAIR. Slice thickness and slice interval were 5.0/1.5 mm. Field of view (FOV) was 240 × 240 mm^2, matrix: 256 × 256. About 0.1 mmol/kg of gadolinium chelate contrast was injected for contrast-enhanced imaging.

T2FLAIR image had rigid registration using CE-T1WI image as a template. Region of interest (ROI) were manually segmented using ITK-SNAP by one neuroradiologist with 15 (***) years experiences. Three tumor sub-region ROIs including the tumor area (the whole body of tumor), peritumoral edema area and contralateral normal healthy white matter area in semioval center were segmented, respectively. The detailed standard of ROI segmentation for the sub-regions is provided in Supplementary Fig. 2.

Subsequently, the CE-T1WI and T2FLAIR images were preprocessed, encompassing N4 correction of bias field, skull stripping, image resampling to 1 × 1 × 1 mm^3 isotropic voxels with a linear interpolator. Inter-scanner harmonization was conducted by normalizing the tumor intensity by minusing the intensity value of contralateral normal healthy white matter. All preprocessing was performed with open source software (Matlab).

2.3. Radiomics feature extraction

The feature pool included 364 radiomics features from the image biomarker standardisation initiative (IBSI) [21], which consisted of intensity, morphological, textural, laws and wavelet features. We extracted the radiomics features from the sub-regions including the tumor area and peritumoral edema area on CE-T1WI and T2FLAIR images, respectively. Thus, a total of 1456 features were obtained.

2.4. Radiomics feature selection and signature construction

All the training radiomics features were normalized by transforming the data into new scores with a mean of 0 and a standard deviation of 1 (z scores), and the test features were normalized with the mean value and standard deviation of training datasets with similar method. The least absolute shrinkage and selection operator (LASSO) Cox regression model was used to select the most useful prognostic radiomics features with non-zero coefficients in training cohort from a subset of uncorrelated predictive features (Supplementary S3). The selected radiomics features were then combined into a radiomics signature (referred as Radio-score) by linear combination of selected radiomics features weighted by their respective coefficients. The hyper parameter was selected using 10-fold cross validation via minimum criteria.

2.5. Validation of radiomics signature

Univariable Cox regression analysis was first performed to investigate the association of Radio-score with OS on both training and test cohorts. The potential association of the radiomics signature with OS was first assessed in training cohort and then validated in test cohort by Kaplan-Meier survival analysis. The patients were classified into high-risk or low-risk groups according to the radiomics score (Radio-score), the threshold of which was identified by X-tile. The difference in the survival curves of the high-risk and low-risk groups was evaluated by log-rank test.

To investigate the relationship between radiomics signature and selected genetic-clinical risk factors in terms of survival benefit, the high and low risk groups divided by radiomics signature were then sub-stratified by the selected genetic-clinical risk factors respectively both in the training and independent test cohorts. The difference in the survival curves of the sub-groups in high-risk or low-risk groups was evaluated by log-rank test.

2.6. Construction and assessment of nomogram

Evaluation of the radiomics signature as an independent biomarker was performed by integrating the following genetic and clinical risk factors into the multivariable Cox proportional hazards model: histologic grade (III or IV), gender (female or male), age, treatment (standard or non-standard), IDH-M (yes or no), and MGMTmet (yes or no), which were also analyzed with univariable Cox regression and Kaplan-Meier survival analysis firstly.

To prove the incremental value of the radiomics signature for individualized assessment of OS in patients with HGG, a nomogram incorporating the radiomics signature and selected independent genetic-clinical risk factors based on the multivariate Cox analysis.

To assess the agreement between the observed outcomes and the OS prediction of nomogram, calibration curves were generated. Furthermore, the Harrell concordance index (C-index) was measured to quantify the discrimination performance.

Finally, a decision curve analysis determined the clinical usefulness

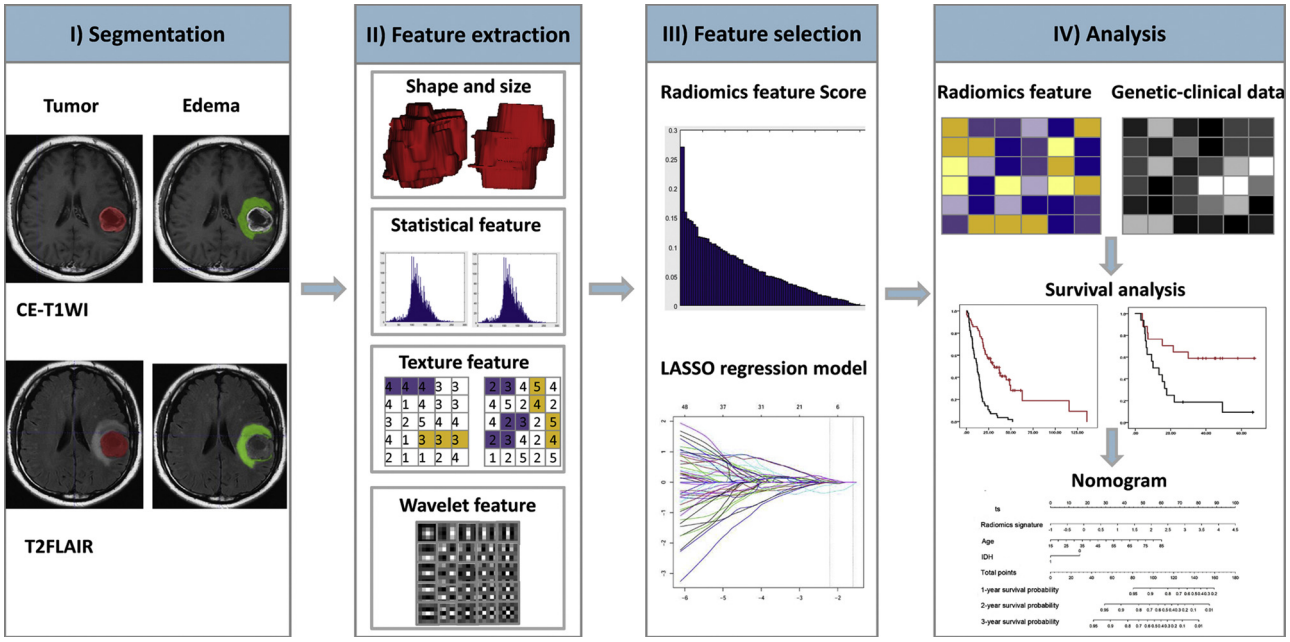

Fig. 1. A flowchart describing the radiomics method for OS prediction. 1) Regions of Interests (ROI) of the tumor lesion and peritumoral edema area were manually delineated, on 2-dimensional CE-T1WI and T2FLAIR images separately. 2) Radiomics features were extracted including non-textural, textural and wavelet features after local standard deviation filter. 3) Discriminative features were selected by the lasso regression model. 4) Prediction model was constructed incorporating the radiomics signature, genetic, and clinical characteristics; a nomogram was finally adopted to present the OS prediction outcomes with a clinical usefulness.

of the nomogram by quantifying the net benefits at different threshold probabilities.

2.7. Statistical analysis

The statistical analysis was performed with R software, version 3.0.1 (http://www.R-project.org) and X-tile software, version 3.6.1 (Yale University School of Medicine, New Haven, Conn). The packages in R used in this study are described as follows: Chi-Squared Test, Mann–Whitney *U* test and Kruskal-Wallis rank sum test were done using the "stats" package. Levene's test was done using the "car" package. Multivariable Cox regression was done using the "glmnet" package. Nomograms and calibration curve were done with the "rms" package. C-index calculation was performed the "Hmisc" package. ROC curves plot was done using "pROC" package. The reported statistical significance levels were all two sided, with the statistical significance level set at 0.05. The differences in age, gender, treatment, histologic grade, IDH-M, MGMTmet, OS between the training and test cohort were assessed by independent samples *t*-test

3. Results

3.1. Clinical and genetic characteristics

Patients' clinical and genetic characteristics in the training and test cohorts are summarized in Table 1. There was no significant difference in age, gender, IDH-M, treatment and OS between the training and independent test cohorts ($P > 0.05$). There were more patients with Grade III ($P < 0.001$), more MGMTmet ($P = 0.024$), and more alive at 2 yrs. ($P = 0.041$) in the independent test cohort compared to those of the training cohort.

3.2. Radiomics signature construction

There were 9, 5, 11 radiomic features in tumor and peritumoral edema area selected with non-zero coefficients in the LASSO Cox regression model for CE-T1WI, T2FLAIR and combined sequences, respectively. The radiomics signature of combined sequences achieved higher C-index (0.707) than that of CE-T1WI (0.700), and T2FLAIR (0.583), respectively (Supplementary S4), and was selected as the final

Table 1
Characteristics of patients in the training and test cohorts.

Characteristic	Training cohort (N = 112)	Test cohort (N = 35)	P
Age (years)			0.588
Range	18 - 81	24 - 77	
Median	56	61	
Mean ± SD	54.44 ± 15.20	56.03 ± 13.31	
Gender, NO. (%)			0.561
Female	54 (48.21)	15 (42.86)	
Male	58 (51.79)	20 (57.14)	
Grade, NO.			< .0001
III (A/O)	38 (18/20#)	24 (24/0)	
IV	74 (66.07)	11 (31.43)	
IDH mutation NO. (%)			0.702
IDH-M	30 (26.79)	11 (31.43)	
IDH-W	82 (73.21)	24 (68.57)	
MGMT met NO. (%)			0.024
MGMTmet	66 (58.93)	27 (77. 14)	
Non-MGMTmet	46 (41.07)	8 (22.85)	
Status NO. (%)			0.041
Alive	19 (16.96)	13 (37.14)	
Dead	93 (83.04)	22 (62.86)	
Treatment NO. (%)			0.056
Standard	98 (87.50)	24 (68.57)	
Non-standard	14 (12.50)	11 (31.43)	
OS (months)			0.353
Range	0.167-135	3.167- 67.4	
Median	16.87	17.77	
Mean ± SD	22.29 ± 20.63	26.11 ± 21.05	

Note: NO.: number; A: astrocytoma; O: oligodendroglioma; # there was no significant difference of OS between astrocytoma and oligodendroglioma; IDH-M: IDH-mutant type; IDH-W: IDH-wild type; MGMTmet: MGMT methylation; Standard: comprehensive treatment included surgery, radiotherapy and/or chemotherapy; NO-Standard: with surgery, but did not get the information of chemotherapy and radiotherapy.

radiomics model. The formula of Radio-score for combined sequences was as follows:

Radio-score (CE-T1WI + T2FLAIR)	= CE-T1WI_Tumor_Mean × 1.092
	+ CE-T1WI_Tumor_Compactness × (-0.033)
	+ CE-T1WI_Tumor_ Angular second moment × (-1.181)
	+ CE-T1WI_Tumor_First measure of information correlation × 1.416
	+ CE-T1WI_Tumor_ Low grey level zone emphasis × (-0.730)
	+ CE-T1WI_Tumor_Wavelet P1L2C2 × 0.015
	+ CE-T1WI_Edema_ Number of connected 3D components × (-0.381)
	+ CE-T1WI_Edema_ Small zone low grey level emphasis × 0.169
	+ CE-T1WI_Edema_Mean intensity × 2.547
	+ T2FLAIR_Edema_Wavelet P1L2C1 × (-0.243)
	+ T2FLAIR_Edema_ Maximum intensity × (-0.053)

3.3. Validation of radiomics signature

Based on the Radio-score of patients in the training cohort, the optimal cutoff calculated by the X-tile plot was 3.315 for Radio-score. Then, patients were stratified into low-risk and high-risk groups by Radio-score, as shown in Fig. 2. The C index of radiomics signature was 0.707 (95%CI, 0.661 to 0.754, $P < .001$) for training cohort, and 0.711 (95%CI, 0.609 to 0.813, $P < .001$) for test cohort. The OS of high risk and low risk groups divided by radiomics signature are showed in Table 2. The patients of low-risk group (OS = 31.1 ± 7.9) survived longer than those of high-risk group (OS = 13.4 ± 3.4).

3.4. Construction and assessment of nomogram

According to univariate Cox regression analysis, the radiomics signature, age, and IDH were significantly associated with OS in both training and test cohorts, as shown in Supplementary S5. The multivariable Cox regression analysis identified radiomics signature, age and IDH as independent risk factors (radiomics signature: HR: 2.18, 95% CI: 1.356–3.513, $P = 0.005$; age: HR: 1.039, 95% CI: 1.019–1.058, $P = 0.005$; and IDH: HR: 0.490, 95% CI: 0.247-0.973, $P = 0.007$).

The low-risk group based on radiomics signature was sub-stratified into subgroups by age (50.5) and IDH respectively, while the high-risk group based on radiomics signature was not sub-stratified by age (60.0) or IDH both in training and independent test cohort (Fig. 3), because most patients were IDH-W (94.6% in training cohort, 88.2% in test cohort), and the mean age was 60.6 ± 12.1 in training cohort, and 61.6 ± 11.9 in test cohort. The OS of subgroup divided by age (50.5) and IDH are showed in Tables 3 and 4 . The MRI images of subgroup are showed in Fig. 4. The greatest survival benefit of HGG was observed in patients with Radio-score < 3.315, IDH-M and age < 50.5, which had an approximately 3-year increased in OS relative to patients in high-risk group (Radio-score ≥ 3.315, IDH-W and age ≥ 60.0).

Based on the relationship of selected risk factors, the nomogram (Fig. 5) was constructed by radiomics signature, age and IDH, and achieved a C-Index of 0.764 (95% CI: 0.723-0.806, $P < .001$) for the training cohort, and 0.758 (95% CI: 0.667-0.838, $P < .001$) for the independent test cohort, demonstrating the improved predictive performance.

The calibration curves of the nomograms for the probability of OS at 1, 2, or 3 years after surgery are shown in Fig. 5. The calibration curves of the nomogram demonstrated satisfactory agreement between the predictive and observational possibility of OS for 1, 2, 3 years in both the training and test cohorts.

A decision curve analysis showed that the nomogram had a higher overall net benefit than the radiomics signature, age and IDH-M across most of the range of reasonable threshold probabilities (Supplementary Fig. 3).

4. Discussion

In the current study, the radiomics signature was identified to be the independent prognostic biomarkers and stratified HGG patients. Age and IDH were important supplements for the low-risk group. The nomogram incorporating the radiomics signature, age and IDH status improved the performance for individualized OS prediction. The greatest survival benefit of HGG was observed in patients with Radio-score < 3.315, IDH-M and age < 50.5, which had an approximately 3-year increased in OS relative to patients in high-risk group (Radio-score ≥ 3.315, IDH-W and age ≥ 60.0).

Our radiomics signature contained 4 texture, 2 tumor shape, 3 first-order and 2 wavelet features from CE-T1WI and T2FLAIR images which could predict the OS of glioma, and stratified patients into high- and low-risk groups in our study. CE-T1WI contains the information of regional angiogenesis in tumor and the destruction of blood-brain barrier.

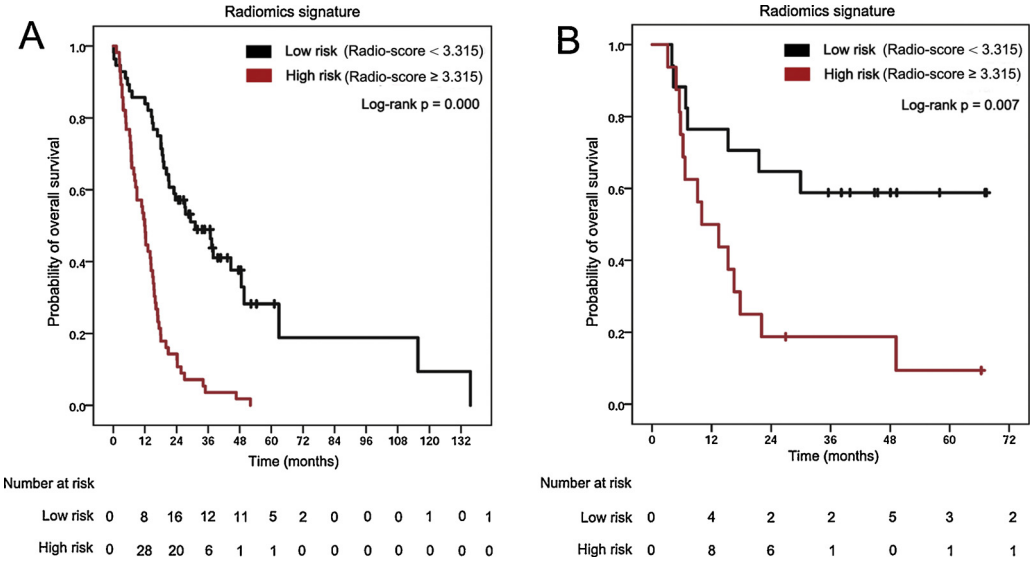

Fig. 2. Kaplan Meier survival analysis of radiomics signature. The radiomics signature successfully stratified HGG into high-risk and low-risk groups with significant prognostic difference, both in training (A), and independent validation cohorts (B).

Table 2
Characteristics of patients according to the risk groups stratified by radiomics signature.

	Training cohort			Test cohort		
	High risk (N = 56)	Low risk (N = 56)	P	High risk (N = 17)	Low risk (N = 18)	P
OS (Months)	13.4 ± 3.4	31.1 ± 7.9	0.000	17.4 ± 4.3	34.3 ± 5.2	0.018
1 year	28 (50.0%)	8 (14.3%)		8 (47.1%)	4 (22.2%)	
2 years	20 (35.7%)	16 (28.6%)		6 (35.3%)	2 (11.1%)	
≥3 years	8 (14.3%)	32 (57.1%)		3 (17.6%)	12(66.7%)	
IDH-M	3 (5.4%)	27 (48.2%)	0.000	2 (11.8%)	9 (50.0%)	0.001
Age	60.6 ± 12.1	48.3 ± 15.5	0.000	61.6 ± 11.9	50.8 ± 12.7	0.016

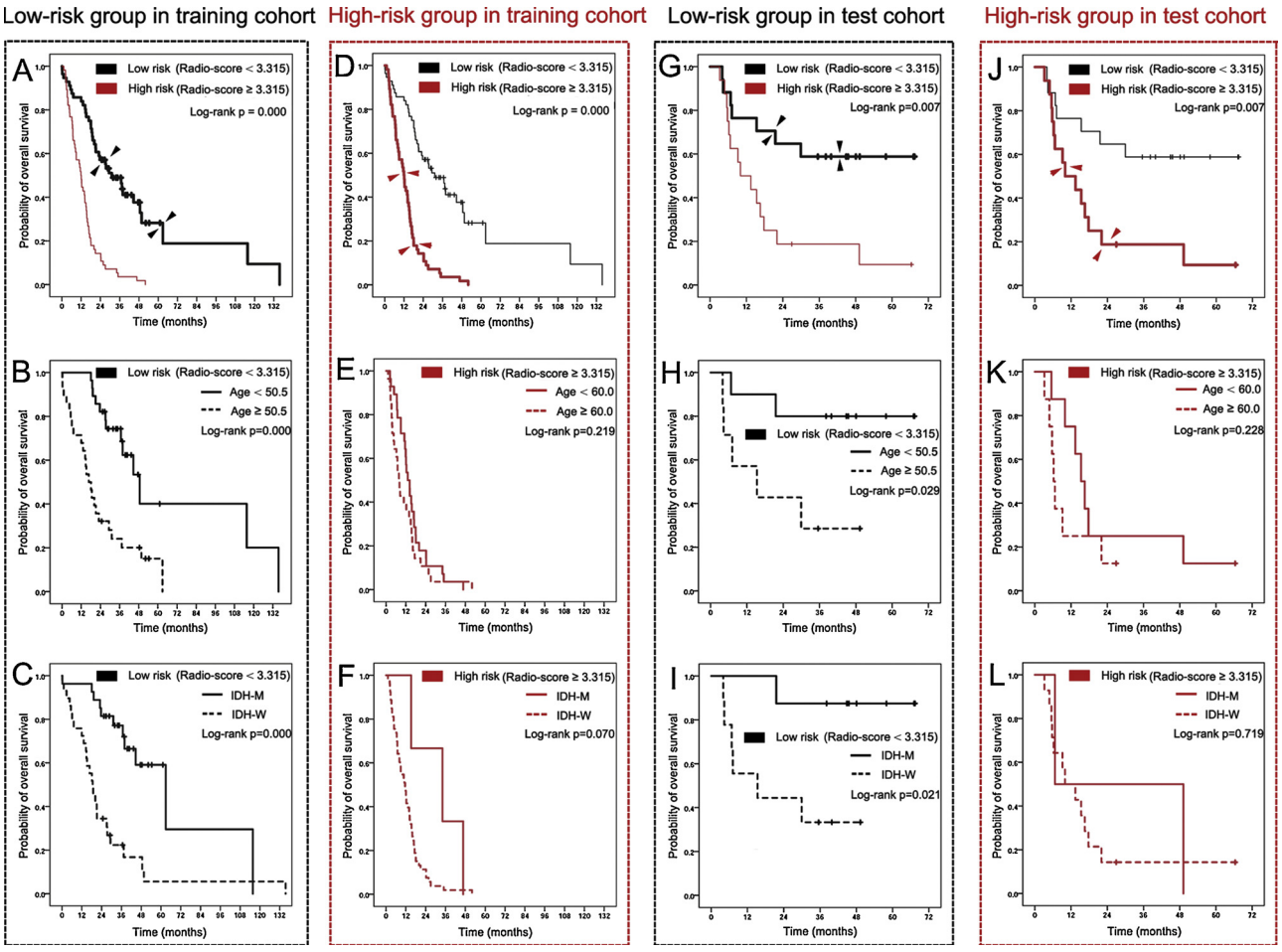

Fig. 3. The sub-stratified analysis by IDH and age based on Kaplan Meier survival analysis of radiomics signature. In low-risk group of radiomics signature, both IDH and age sub-stratified patients into two subgroup in training (A–C) and independent validation cohorts (G–I). In high-risk group of radiomics signature, both IDH and age failed to sub-stratify patients in training (D–F) and independent validation cohorts (J–L).

Table 3
The subdivided analyses by age in high and low risk groups based on radiomics signature.

	Training cohort						Test cohort					
	High risk (N = 56)			Low risk (N = 56)			High risk (N = 17)			Low risk (N = 18)		
	Age ≥ 60 (N = 28)	Age < 60 (N = 28)	*P*	Age ≥ 50.5 (N = 28)	Age < 50.5 (N = 28)	*P*	Age ≥ 60 (N = 9)	Age < 60 (N = 8)	*P*	Age ≥ 50.5 (N = 8)	Age < 50.5 (N = 10)	*P*
OS (Months)	11.4 ± 2.0	15.5 ± 1.9	0.147	21.6 ± 3.4	40.7 ± 5.0	0. 002	10.6 ± 3.1	24.3 ± 7.6	0.130	20.8 ± 6.7	43.7 ± 6.0	0.023
1 year	17 (60.7%)	11 (39.3%)	–	8 (28.6%)	0 (0.0%)	–	7 (77.8%)	2 (25.0%)	–	4 (50.0%)	1 (10.0%)	–
2 years	8 (28.6%)	12 (42.9%)	–	10 (35.7%)	5 (17.9%)	–	1 (11.1%)	4 (50.0%)	–	1 (12.5%)	1 (10.0%)	–
≥3 years	3 (10.7%)	5 (17.8%)	–	10 (35.7%)	23 (82.1%)	–	1 (11.1%)	2 (25.0%)	–	3 (37.5%)	8 (80.0%)	–
IDH-M	0	3		7	20		1	1		0	9	

Table 4
The subdivided analyses by IDH in high and low risk groups based on radiomics signature.

	Training cohort						Test cohort					
	High risk (N = 56)			Low risk (N = 56)			High risk (N = 17)			Low risk (N = 18)		
	IDH-W (N = 53)	IDH-M (N = 3)	*P*	IDH-W (N = 29)	IDH-M (N = 27)	*P*	IDH-W (N = 15)	IDH-M (N = 2)	*P*	IDH-W (N = 9)	IDH-M (N = 9)	*P*
OS (Months)	12.4 ± 9.0	32.0 ± 9.1	0.163	23.3 ± 4.7	39.5 ± 4.0	0. 011	15.9 ± 4.3	27.9 ± 21.3	0.673	21.4 ± 5.8	48.8 ± 5.4	0.004
1 year	27 (50.9%)	0 (0.0%)	–	8 (27.6%)	1 (3.7%)	–	8 (53.4%)	1 (50.0%)	–	4 (44.4%)	0 (0.0%)	–
2 years	20 (33.8%)	0 (0.0%)	–	11 (37.9%)	4 (14.8%)	–	5 (33.3%)	0 (0.0%)	–	1 (11.2%)	2 (22.2%)	–
≥3 years	6 (11.3%)	3 (100%)	–	10 (34.5%)	22 (81.5%)	–	2 (13.3%)	1 (50.0%)	–	4 (44.4%)	7 (77.8%)	–
Age	61.5 ± 11.4	44.3 ± 8.1	0.163	55.5 ± 14.3	40.5 ± 13.1	0.000	63.1 ± 9.1	51.0 ± 20	0.652	57.8 ± 11.1	42.8 ± 9.3	0.008

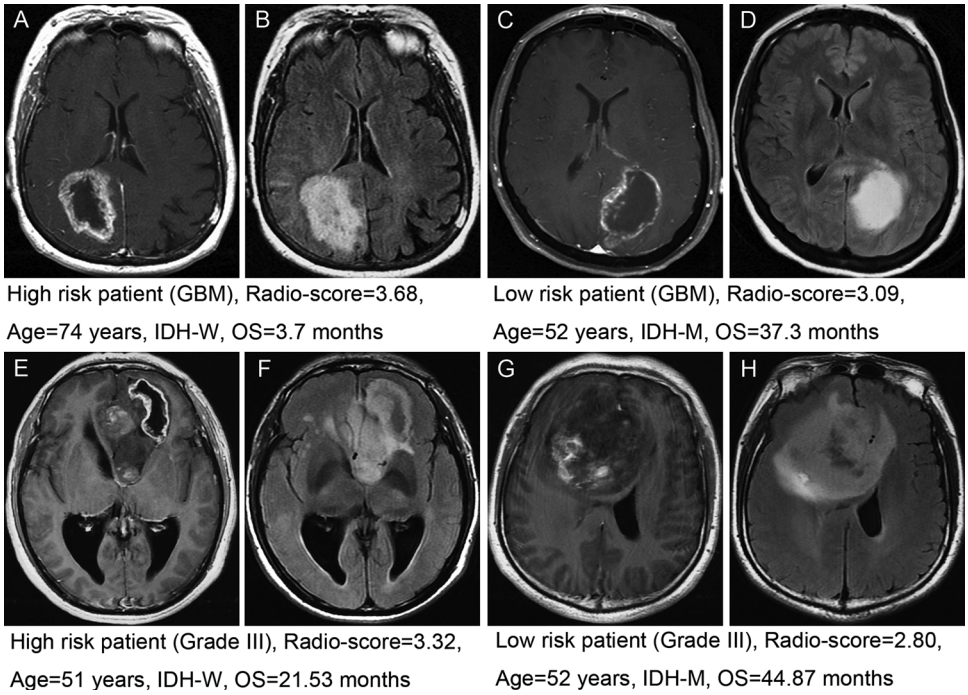

Fig. 4. MRI images of HGG in high-risk and low-risk patients. Both glioblastomas (GBMs) showed ring enhancement (A–D), but one patient (A, B) was stratified to high risk group (Radio-score = 3.68; age = 74 years; IDH-W; OS = 3.7 months), the other patient (C, D) was stratified to low risk group (Radio-score = 3.09; age = 52 years; IDH-M; OS = 37.3 months). Both Grade III gliomas showed irregular enhancement near midline (E–H), but one patient (E, F) was stratified to high risk group (Radio-score = 3.32; age = 51 years; IDH-W; OS = 21.53 months), the other patient (G, H) was stratified to low risk group (Radio-score = 2.80; age = 52 years; IDH-M; OS = 44.87 months). Note: A, C, E, G represented the CE-T1WI images; B, D, F, H represented the T2FLAIR images.

T2FLAIR reflects the anatomical information and density of tumor cells. The radiomics features from these two sequences could quantify the comprehensive information to characterize the heterogeneity of the glioma [11,12], [15]. Previous studies have confirmed the hypothesis that the prognostic information could be inferred from the radiological images of glioma [13,14,22]. Chaddad A, et al. [23] showed that the texture features could characterize the heterogeneity of GBM and predict the OS. Liu Y, et al. [24] showed that radiomics could reflect heterogeneous distribution of GBM and thereby affect the survival stratification. Li QH, et al. [25] found that the multiparametric radiomics signature had the potential to offer better prognostic performance for GBM. Furthermore, we confirmed that the combined 11 radiomics features could accurately reflect this whole heterogeneous information of angiogenesis and cell proliferation both in tumor and edema regions which are closely related to the prognosis of HGG.

The multivariable Cox regression analysis identified radiomics signature, age and IDH as independent risk factors. We further analyzed the relationship between radiomics signature, age and IDH status. In high-risk group stratified by radiomics signature, there was no subgroups existing by the sub-stratified analysis of IDH and age, respectively. This demonstrated that the radiomics signature was an enough noninvasive imaging biomarker for high-risk group, and partly reflecting the information of IDH status and age, because most patients of this group were IDH-W (94.6%) and the mean age was 60.6 years old. It confirms that IDH mutations can convert α-ketoglutarate to 2-hydroxyglutarate, which ultimately suppresses angiogenesis and cell proliferation [26]. The radiomics signature from CE-T1WI and T2FLAIR images could reflect the biological processes of high-risk group. While in low-risk group, patients were successfully sub-stratified into subgroups by IDH and age, respectively. The patients with IDH-M and age < 50.5 survived longer than those with IDH-W and age ≥ 50.5. Thus, age and IDH were important supplements to radiomics signature for low-risk group. Our study first expands on the knowledge by demonstrating a relationship between radiomics signature, IDH and age in terms of survival benefit.

The complex nature of tumor malignancy might be better reflected when considering the interactions between the multiple risk factors [27,28]. The nomogram which takes account of multiple risk factors by assigning a total number of points to each patient, is imperative [12,29–31]. A recent study integrating radiomics features, age, and KPS successfully improved the performance of OS prediction for GBM [32]. The 2016 WHO Classification of Tumors of the Central Nervous System firstly defines the IDH genotype of glioma, which is an important genetic hallmark with considerable prognostic value [33,34]. Given the relationship between radiomics signature, IDH and age in our study, we combined these variables into a nomogram, and the predictive power was improved with C-index of 0.764, which demonstrated the incremental value of combining multiple variables for individualized OS prediction in HGG patients. The greater survival benefit of HGG patients was observed in low-risk group (Radio-score < 3.315, IDH-M and

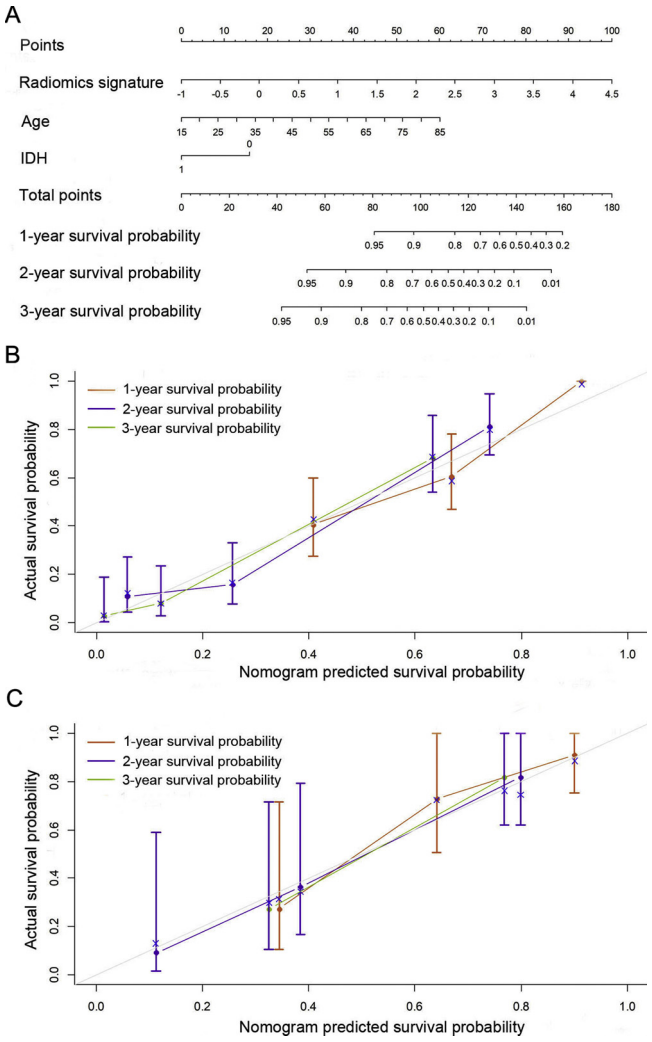

Fig. 5. The nomogram constructed by radiomics signature, IDH and age (A). The calibration curves of the nomogram demonstrated satisfactory agreement between the predictive and observational possibility in both the training (B) and test cohorts (C).

age < 50.5), which had an approximately 3-year increased in OS relative to patients in high-risk group (Radio-score ≥ 3.315, IDH-W and age ≥ 60.0). Thus, the patients in low-risk group would be strongly recommended with current standard therapy to obtain the survival benefit, while the patients in high-risk group might be better to add other more aggressive treatments such as immunotherapy or targeted therapy. Our nomogram provided a robust method to address the survival estimation for HGG, which might be a new complement to the treatment guidelines of glioma for clinical use.

There were still several limitations in our study. First, we used the retrospective data with relatively small sample size, although independent test cohort was included. Multi-center data should be collected to test the stable performance of the model. Secondly, because the heterogeneity of imaging parameters in the TCIA cohort, we only included the routine sequences (CE-T1WI and T2FLAIR) and did not investigate the advanced MR sequences. Thirdly, some variables, such as extent of resection and KPS, were not available for the patients from TCGA. We excluded the patients with biopsy.

5. Conclusions

In conclusion, the radiomics signature is an independent prognostic biomarker for HGG, and successfully stratified patients. Age and IDH were important supplements for radiomics signature, especially for the low-risk group. A nomogram incorporating radiomics signature, IDH and age improved the performance of individualized OS estimation, which might be a new complement to the treatment guidelines of glioma for clinical use.

Declaration of Competing Interest

The authors declare that they have no potential conflicts of interest.

Acknowledgements

This study was supported by the National Natural Science Foundation [grant numbers 81471652, 81771824, 81701681]; the Precision Medicine Key Innovation Team Project [YT1601].

Appendix A. Supplementary data

Supplementary material related to this article can be found, in the online version, at doi:https://doi.org/10.1016/j.ejrad.2019.07.010.

References

[1] T.W. Wang, X.D. Niu, T. Gao, et al., Prognostic Factors for Survival Outcome of High-Grade Multicentric Glioma, World Neurosurgery, 2018, https://doi.org/10.1016/j.wneu.2018.01.035.
[2] R. Stupp, M.E. Hegi, W.P. Mason, et al., Effects of radiotherapy with concomitant and adjuvant temozolomide versus radiotherapy alone on survival in glioblastoma in a randomised phase III study: 5-year analysis of the EORTC-NCIC trial, Lancet Oncol. 10 (2009) 459–466.
[3] N. Sanai, M.S. Berger, Surgical oncology for gliomas: the state of the art, Nat. Rev. Clin. Oncol. 15 (2018) 112–125.
[4] E.G. Van Meir, C.G. Hadjipanayis, A.D. Norden, H.K. Shu, P.Y. Wen, J.J. Olson, Exciting new advances in Neuro-Oncology: the avenue to a cure for malignant glioma, CA Cancer J. Clin. 60 (2010) 166–193.
[5] J. Scott, N. Rewcastle, P. Brasher, et al., Which glioblastoma multiforme patient will become a long term survivor? A population based study, Ann Neurology 46 (1999) 183–188.
[6] R. Sawaya, M. Hammoud, D. Schoppa, et al., Neurosurgical outcomes in a modern series of 400 craniotomies for treatment of parenchymal tumors, Neurosurgery 42 (5) (1998) 1044–1055.
[7] C.B. Schechter, Brain and other central nervous system cancers: recent trends in incidence and mortality, J. Natl. Cancer Inst. 91 (23) (1999) 2050–2051.
[8] J. Bruce, B. Kennedy, H. Engelhard, et al., Glioblastoma Multiforme: Practice Essentials, Background, Pathophysiology. [online] Emedicine.medscape.com, Available at: (2017) http://emedicine.medscape.com/article/283252-overview.
[9] J.C. Peeken, J. Hesse, B. Haller, K.A. Kessel, F. Nusslin, S.E. Combs, Semantic imaging features predict disease progression and survival in glioblastoma multiforme patients, Contemp. Oncol. Pozn. (Pozn) 22 (1A) (2018) 81–85.
[10] H. Zhou, M. Vallières, H.X. Bai, et al., MRI features predict survival and molecular markers in diffuse lower-grade gliomas, Neuro Oncol 19 (6) (2017) 862–870.
[11] S.A. Keek, R.T.H. Leijenaar, A. Jochems, H.C. Woodruff, A review on radiomics and the future of the theragnostics for patient selection in precision medicine, Br. J. Radiol. (2018), https://doi.org/10.1259/bjr.20170926.
[12] B. Altazi, D. Fernandez, G. Zhang, M. Biagioli, E. Moros, H.L. Moffitt, SU-E-J-258: prediction of cervical cancer treatment response using radiomics features based on F18-FDG uptake in PET images, Med. Phys. 42 (6) (2015) 3326.
[13] P. Kickingereder, S. Burth, A. Wick, et al., Radiomic profiling of glioblastoma: identifying an imaging predictor of patient survival with improved performance over established clinical and radiologic risk models, Radiology 280 (3) (2016) 880–889.
[14] S. Rathore, H. Akbari, M. Rozycki, et al., Radiomic MRI signature reveals three distinct subtypes of glioblastoma with different clinical and molecular characteristics, offering prognostic value beyond IDH1, Sci. Rep. 8 (2018) 5087.
[15] Y.Q. Huang, Z.Y. Liu, L. He, et al., Radiomics signature: a potential biomarker for the prediction of disease-free survival in early-stage (I or II) non–small cell lung Cancer, Radiology 281 (3) (2016) 947–957.
[16] K.T. Carroll, A.K. Bryant, B. Hirshman, et al., Interaction between the contributions of tumor location, tumor grade, and patient age to the survival benefit associated with gross total resection, World Neurosurg. (2018) e790–e798, https://doi.org/10.1016/j.wneu.2017.12.165.
[17] B. Czapski, S. Baluszek, C. Herold-Mende, B. Kaminska, Clinical and immunological correlates of long term survival in glioblastoma, Contemp. Oncol. Pozn. (Pozn) 22 (1A) (2018) 81–85.
[18] M. Shirahata, T. Ono, D. Stichel, et al., Novel, improved grading system(s) for IDH-mutant astrocytic gliomas, Acta Neuropathol. 136 (2018) 153–166.
[19] D. Valiyaveettil, M. Malik, D. Joseph, S.F. Ahmed, S.A. Kothwal, Prognostic factors and outcomes in anaplastic gliomas: an institutional experience, South Asian J. Cancer 7 (1) (2018) 1–4.

[20] Jan C. Buckner, Factors influencing survival in high-grade gliomas, Semin. Oncol. 30 (6) (2003) 10–14.
[21] S.L. Alex Zwanenburg, Martin Vallières, Steffen Löck, Image biomarker standardisation initiative, arXiv (2017) 161207003.
[22] R.J. Gillies, P.E. Kinahan, H. Hricak, Radiomics: images are more than Pictures, they are Data, Radiology 278 (2016) 563–577.
[23] A. Chaddad, S. Sabri, T. Niazi, B. Abdulkarim, Prediction of survival with multi-scale radiomic analysis in glioblastoma patients, Med. Biol. Eng. Comput. (2018), https://doi.org/10.1007/s11517-018-1858-4.
[24] Y. Liu, X. Zhang, N. Feng, et al., The effect of glioblastoma heterogeneity on survival stratification: a multimodal MR imaging texture analysis, Acta radiol. (2018), https://doi.org/10.1177/0284185118756951.
[25] Q.H. Li, H. Bai, Y.S. Chen, et al., A fully-automatic multiparametric radiomics model: towards reproducible and prognostic imaging signature for prediction of overall survival in glioblastoma multiforme, Sci. Rep. 7 (2017) 14331.
[26] L. Dang, K. Yen, E.C. Attar, IDH mutations in cancer and progress toward development of targeted therapeutics, Ann. Oncol. 27 (4) (2016) 599–608.
[27] J.W. Lao, Y.S. Chen, Z.C. Li, et al., A deep learning-based radiomics model for prediction of survival in glioblastoma multiforme, Sci. Rep. (2017), https://doi.org/10.1038/s41598-017-10649-87.
[28] G.S. Collins, J.B. Reitsma, D.G. Altman, K.G. Moons, Transparent reporting of a multivariable prediction model for individual prognosis or diagnosis (TRIPOD): the TRIPOD statement, Ann. Intern. Med. 162 (1) (2015) 55–63.
[29] H. Gittleman, D. Lim, M.W. Kattan, et al., An independently validated nomogram for individualized estimation of survival among patients with newly diagnosed glioblastoma: NRG Oncology RTOG 0525 and 0825, Neuro Oncol 19 (5) (2017) 669–677.
[30] W. Liang, L. Zhang, G. Jiang, et al., Development and validation of a nomogram for predicting survival in patients with resected non-small-cell lung cancer, J. Clin. Oncol. 33 (8) (2015) 861–869.
[31] Y. Chen, Y. Zhang, W. Yang, et al., Accuracy of a nomogram to predict the survival benefit of surgical axillary staging in T1 breast cancer patients, Medicine (Baltimore) 97 (26) (2018) e11273.
[32] J. Lao, Y. Chen, Z.C. Li, et al., A deep learning-based radiomics model for prediction of survival in glioblastoma multiforme, Sci. Rep. 7 (1) (2017) 10353.
[33] K. Ichimura, Y. Narita, C.E. Hawkins, Diffusely infiltrating astrocytomas: pathology, molecular mechanisms and markers, Acta Neuropathol. 129 (6) (2015) 789–808.
[34] D.N. Louis, A. Perry, G. Reifenberger, et al., The 2016 world health organization classification of tumors of the central nervous system: a summary, Acta Neuropathol. 131 (6) (2016) 803–820.